Organic & Biomolecular Chemistry

Accepted Manuscript

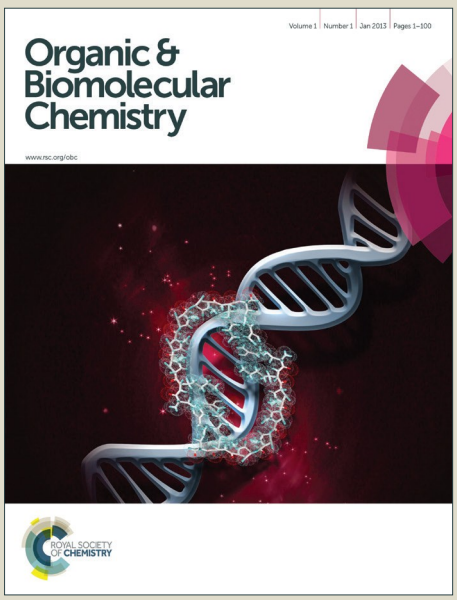

ROYAL SOCIETY OF CHEMISTRY

www.rsc.org/obc

Locked Nucleic Acid (LNA) induced effect on hybridization and fluorescence properties of oligodeoxyribonucleotides modified with nucleobase-functionalized DNA monomers†

Mamta Kaura and Patrick J. Hrdlicka*

Department of Chemistry, University of Idaho, Moscow, ID 83844-2343, USA

*Corresponding author: Phone: (+1) 208 885 0108. Fax: (+1) 208 885 6173. Email: hrdlicka@uidaho.edu.

ABSTRACT. LNA and nucleobase-modified DNA monomers are two families of building blocks, which are used extensively in oligonucleotide chemistry. However, there are only very few reports in which these two monomer families are used alongside of each other. In the present study we set out to characterize the biophysical properties of oligodeoxyribonucleotides in which C5-modified 2′-deoxyuridine or C8-modified 2′-deoxyadenosine monomers are flanked by LNA nucleotides. We hypothesized that the LNA monomers would alter the sugar rings of the modified DNA monomers toward more RNA-like *North*-type conformations for maximal DNA/RNA affinity and specificity. Indeed, incorporation of LNA monomers almost invariably results in increased target affinity and specificity relative to the corresponding LNA-free ONs, but the magnitude of the stabilization varies greatly. Introduction of LNA nucleotides as direct neighbors to C5-pyrene-functionalized pyrimidine DNA monomers yields oligonucleotide probes with more desirable photophysical properties as compared to the corresponding LNA-free probes, including more intense fluorescence emission upon target binding and improved discrimination of single nucleotide polymorphisms (SNPs). These hybrid oligonucleotides therefore present themselves as promising probes for diagnostic applications.

INTRODUCTION. Locked nucleic acids (LNAs) are a class of conformationally restricted nucleotides that are extensively used in oligonucleotide chemistry to increase affinity against complementary DNA/RNA (cDNA/cRNA), improve discrimination of mismatched targets, and confer protection against enzymatic degradation (Figure 1).[1-3] The interesting properties of LNA-modified oligonucleotides has led to their widespread use in molecular biology, nucleic acid diagnostics, and antisense technology,[3,4] and has stimulated development of many closely related analogs,[5,6] including LNAs with modified nucleobase moieties.[7-9] C5-alkynyl-modified LNA pyrimidines are particularly interesting building blocks as their incorporation into oligonucleotides promotes additional increases in cDNA/cRNA affinity, specificity and enzymatic stability relative to canonical LNA probes.[7]

In the present work, we set out to study if oligodeoxyribonucleotides (ONs), in which nucleobase-modified DNA monomers are flanked by canonical LNA nucleotides, emulate the biophysical properties of nucleobase-modified LNA. Previous studies have demonstrated that LNA monomers - themselves featuring a sugar ring that is conformationally restricted in a *North*-type C3′-*endo* conformation - shift the furanose rings of flanking nucleotides toward more pronounced *North*-type conformations.[10] We therefore hypothesized that LNA monomers can shift the conformations of proximal nucleobase-modified DNA monomers toward similar *North*-type conformations as adopted by nucleobase-modified LNA. A similar strategy has been used to modulate the properties of ONs modified with N2′-functionalized 2′-aminouridines,[11] 1-(phenylethynyl)pyrene-functionalized 2′-arabinouridines[12] or – more recently – 2′-*O*-(pyren-1-yl)methyluridines.[13]

This potential strategy to nucleobase-modified LNA is appealing due to the commercial availability of canonical LNA phosphoramidites and nucleobase-modified DNA phosphoramidites. Toward this end, we set out to synthesize and characterize the biophysical properties of ONs, in which representative C5-alkynyl-functionalized pyridine DNA monomers **W**-**Z**[14] or C8-alkynyl-functionalized purine DNA monomers **L**-**N**[14e,15] are flanked by LNA nucleotides (Figure 1).

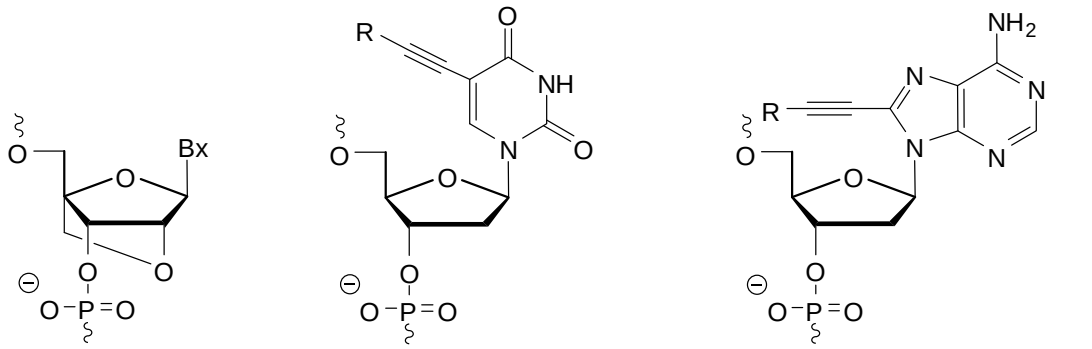

LNA

Monomer W R: -H
Monomer X R: -CH_2NH_2
Monomer Y R: -Py
Monomer Z R: -$CH_2NHCOPy$

Monomer L R: -H
Monomer M R: -Py
Monomer N R: -$CH_2NHCOPy$

Figure 1. Structures of LNA, C5-functionalized 2′-deoxyuridines and C8-functionalized 2′-deoxyadenosines studied herein.

RESULTS AND DISCUSSION.

Synthesis of nucleobase-functionalized DNA phosphoramidites. The corresponding phosphoramidites of the C5-functionalized 2′-deoxyuridine monomers **W**-**Z** were obtained as described in the literature,[14b,14h,16-18] while the C8-functionalized 2′-deoxyadenosine phosphoramidites were prepared as outlined in Schemes 1 and 2. Thus, known 8-bromo 2′-deoxyadenosine derivative **1**[19] was coupled to *N*-(prop-2-ynyl)pyrene-1-carboxamide using Sonogashira conditions to provide nucleoside **2** in 50% yield (Scheme 1). Subsequent O3′-phosphitylation, using 2-cyanoethyl *N*,*N*-diisopropylchlorophosphoramidite (PCl reagent) and *N*,*N*-diisopropylethylamine (DIPEA), afforded target phosphoramidite **3N** in 60% yield.

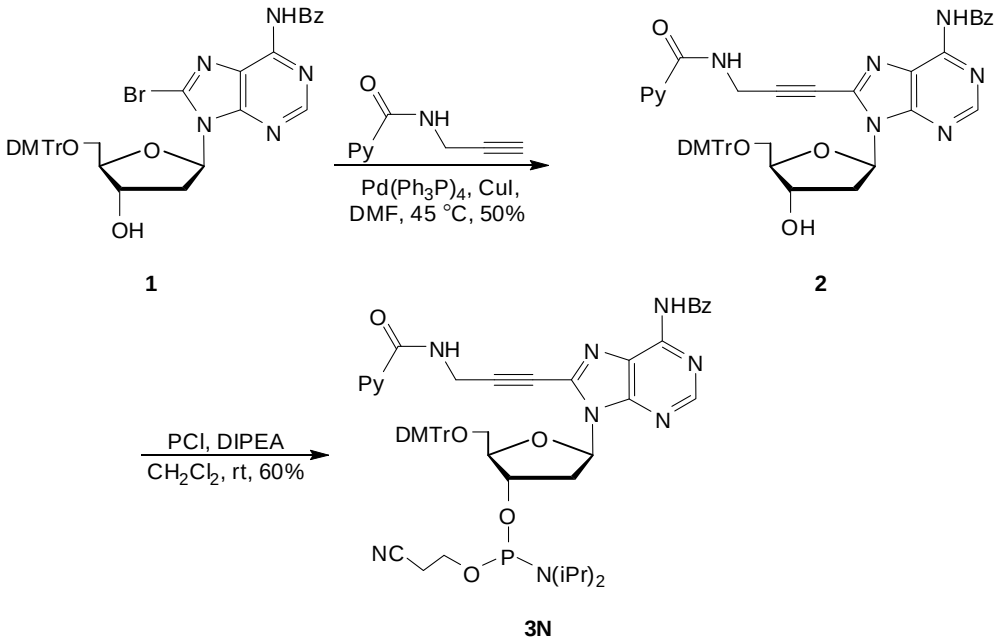

Scheme 1. Synthesis of C8-functionalized 2′-deoxyadenosine **3N**. PCl reagent = 2-cyanoethyl-*N*,*N*-diisopropylchlorophosphoramidite; DIPEA = *N*,*N*-diisopropylethylamine.

The reaction sequence for the synthesis of phosphoramidites **3L** and **3M** was modified as Sonogashira couplings between nucleoside **1** and trimethylsilylacetylene or 1-ethynylpyrene[20]

were sluggish, resulting in incomplete reactions and low reaction yields. Nucleoside **4**[21], featuring an unprotected adenine moiety, was found to be a more suitable substrate for Sonogashira couplings, providing nucleosides **5L** and **5M** in 68% and 80% yield, respectively (Scheme 2). Attempts to benzoylate the N6-position using a transient protection protocol[22] were not satisfactory and the exocyclic amine of the adenine moiety was instead protected as an *N*,*N*-dimethylformamidine group[23] to afford nucleosides **6L** and **6M** in 83% and 87% yield, respectively. Subsequent O3′-phosphitylation provided target nucleosides **3L** and **3M** in 72% and 64% yield, respectively.

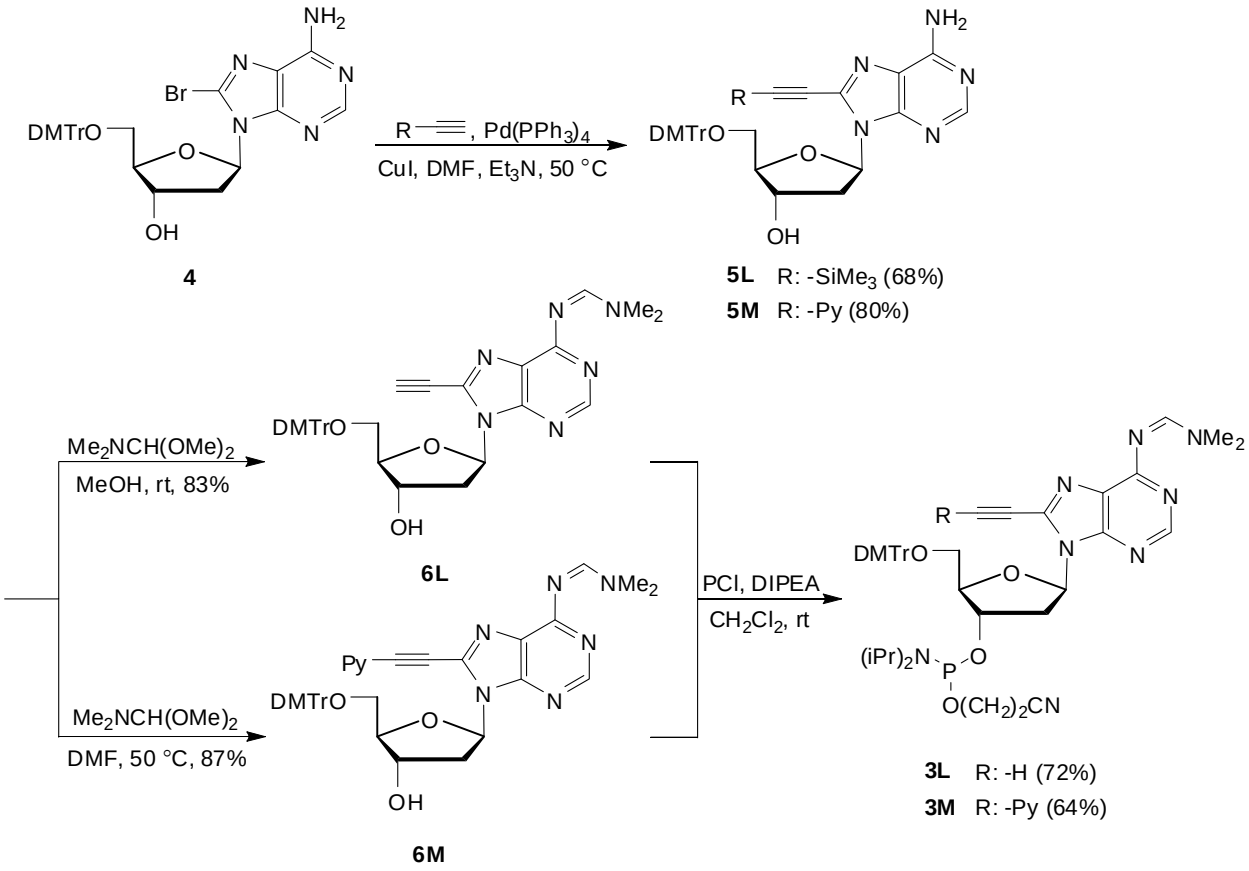

Scheme 2. Synthesis of C8-functionalized 2′-deoxyadenosines **3L** and **3M**.

Oligonucleotide synthesis. Nucleobase-modified phosphoramidites were used to prepare 9-mer ONs in which monomers **L**/**M**/**N**/**W**/**X**/**Y**/**Z** were incorporated with LNA nucleotides as direct (**B2**/**B5** series) or next-nearest neighbors (**B3**/**B6** series) (Tables 1 and 2). In addition, LNA-free ONs (**B1**/**B4** series) were synthesized as controls. ONs with a central incorporation of monomer **W** monomer are referred to as the **W**-series. Similar conventions apply for ONs modified with other monomers. Reference ONs, in which the central thymidine or 2′-deoxyadenosine is unmodified, are referred to as **T1**-**T3** and **A4**-**A6** series, respectively (Tables 1 and 2). For unabridged ON nomenclature, see Table S1.

The following conditions, which were identified from a screen of typical activators, were used during machine-assisted solid-phase DNA synthesis (activator/coupling time/coupling yield): 5-(ethylthio)-1*H*-tetrazole/20 min/~95% (monomers **M**/**N**), 4,5-dicyanoimidazole/20 min/~95% (monomers **L**/**W**/**X**) and 5-[3,5-bis(trifluoromethyl)phenyl]-1*H*-tetrazole/20 min/~95% (monomers **Y**/**Z** and canonical LNA monomers). The composition and purity of all modified ONs was verified by MALDI-MS/MS analysis (Table S1) and ion-pair reverse-phase HPLC respectively.

Hybridization with cDNA/cRNA targets. Thermal denaturation temperatures (T_m's) of duplexes between ONs and complementary DNA and RNA (cDNA/cRNA) were determined in medium salt buffer ([Na^+] = 110 mM, pH 7.0). All denaturation curves exhibited sigmoidal monophasic transitions (Figure S1).

As expected,[14a-14d] ONs that are modified with C5-ethynyl- or C5-aminopropynyl-functionalized 2′-deoxyuridine monomers **W** and **X** display moderately increased affinity toward cDNA and cRNA relative to unmodified reference ONs due to the larger π-surface area and/or

protonated nature of these monomers (ΔT_m for **W1** and **X1** up to +5 °C, Table 1). In contrast, ONs that are modified with bulky pyrene-functionalized monomers **Y** and **Z** display greatly reduced cDNA/cRNA affinity (ΔT_m for **Y1** and **Z1** down to -11 °C, Table 1). Previous reports have ascribed the destabilization to the steric bulk and/or hydrophobicity of the pyrene moieties, which likely perturb the hydration spine of the duplexes.[14e-14i]

ONs, in which two LNA nucleotides are incorporated as flanking or next-nearest neighbors relative to C5-ethynyl-2′-deoxyuridine monomer **W**, exhibit very high affinity toward cDNA and cRNA (ΔT_m between +7.5 °C and +17.5 °C, Table 1). However, the affinity-enhancing effects of the LNA and **W** monomers are not additive (note that the ΔT_m of **W2** is less than the sum of ΔT_m's observed for **T2** and **W1**, Table 1). ONs with LNA nucleotides near C5-aminopropynyl-2′-deoxyuridine monomer **X** display even higher cDNA/cRNA affinity but the effects on duplex stability upon mixing these two chemistries are variable; synergistic stabilization is observed for **X3** vs cDNA, additive stabilization is observed for **X2** vs cDNA and **X3** vs cRNA, while less-than-additive stabilization is seen for **X2** vs cRNA (Table 1). Thus, the stabilizing influence that LNA nucleotides exert on nearby C5-modified DNA monomers appears to depend on the distance between the modifications and the type of duplex formed.

Introduction of LNA nucleotides in the vicinity of **Y** and **Z** monomers generally only results in small cDNA affinity increases relative to LNA-free ONs, while much more substantial increases in cRNA affinity are observed (e.g., compare ΔT_m of **Y2** vs cDNA and cRNA, Table 1). Presumably, these trends reflect different geometrical preferences, i.e., LNA nucleotides are known to tune duplex geometries toward more RNA:RNA-like geometries,[10a] while **Y** and **Z** monomers prefer more DNA:DNA-like geometries (compare ΔT_m of **T2** vs cDNA and cRNA, relative to **Y1** and **Z1**, Table 1).

Table 1. Thermal denaturation data for duplexes between ONs modified with C5-functionalized pyrimidine monomers **W**-**Z** and complementary DNA or RNA.[a]

			T_m (ΔT_m) / °C									
			cDNA: 3′-CAC TAT ACG					cRNA: 3′-CAC UAU ACG				
ON	**Sequence**	**B =**	T	**W**	**X**	**Y**	**Z**	T	**W**	**X**	**Y**	**Z**
B1	5′-GTG A**B**A TGC		29.5	31.0 (+1.5)	32.0 (+2.5)	22.5 (-7.0)	22.5 (-7.0)	27.0	30.0 (+3.0)	32.0 (+5.0)	16.0 (-11.0)	16.0 (-11.0)
B2	5′-GTG **aBa** TGC		38.5 (+9.0)	37.0 (+7.5)	41.0 (+11.5)	23.5 (-6.0)	21.5 (-8.0)	43.0 (+16.0)	42.0 (+15.0)	44.5 (+17.5)	34.0 (+7.0)	32.0 (+5.0)
B3	5′-GT**g** A**B**A **t**GC		39.5 (+10.0)	37.5 (+8.0)	44.5 (+15.0)	26.0 (-3.5)	31.5 (+2.0)	47.5 (+20.5)	46.0 (+19.0)	52.5 (+25.5)	29.0 (+2.0)	35.0 (+8.0)

[a] ΔT_m = change in T_m′s relative to unmodified reference duplexes. T_m's determined as the first derivative maximum of denaturation curves (A_{260} vs T) recorded in medium salt buffer ($[Na^+]$ = 110 mM, $[Cl^-]$ = 100 mM, pH 7.0 (NaH_2PO_4/Na_2HPO_4)), using 1.0 μM of each strand. T_m's are averages of at least two measurements within 1.0 °C. A/C/G/T = adenin-9-yl/cytosin-1-yl/guanin-9-yl/thymin-1-yl DNA monomers. LNA modifications are shown in lower case. See Figure 1 for structures of monomers **W**-**Z**.

Incorporation into ONs of C8-ethynyl 2′-deoxyadenosine monomer **L** and, especially, C8-pyrene-functionalized monomers **M** and **N**, results in greatly reduced cDNA/cRNA affinity (see ΔT_m for **L4**-**N4**, Table 2).[14e,15] The affinity-decreasing effects of monomer **L** are compensated by proximal LNA nucleotides (note that the ΔT_m for **L5** is similar to the sum of ΔT_m's for **A5** and **L4**, Table 2). The effects on binding affinity upon incorporation of LNA nucleotides and C8-pyrene-functionalized 2′-deoxyadenosine monomers **M** and **N** into ONs, on the other hand, are more complex. Thus, introduction of neighboring LNA nucleotides fully reverses the destabilizing effect of monomers **M** and **N**, while LNA nucleotides positioned as next-nearest neighbors have a very limited stabilizing effect (Table 2).

Table 2. Thermal denaturation data for duplexes between ONs modified with C8-functionalized purine monomers **L**-**N** and complementary DNA or RNA.[a]

			T_m (ΔT_m) / °C							
			DNA: 3′-CGT ATA GTG				RNA: 3′-CGU AUA GUG			
ON	**Sequence**	**B =**	A	**L**	**M**	**N**	A	**L**	**M**	**N**
B4	5′-GCA T**B**T CAC		29.5	24.5 (-5.0)	17.5 (-12.0)	14.0 (-15.5)	27.0	25.0 (-2.0)	<15.0 (<-12.0)	20.0 (-7.0)
B5	5′-GCA t**B**t CAC		41.5 (+12.0)	36.0 (+6.5)	29.5 (±0.0)	29.0 (-0.5)	40.5 (+13.5)	38.5 (+11.5)	32.0 (+5.0)	31.0 (+4.0)
B6	5′-GCa T**B**T cAC		38.5 (+9.0)	34.0 (+4.5)	20.5 (-9.0)	17.0 (-12.5)	40.5 (+13.5)	40.0 (+13.0)	29.0 (+2.0)	15.0 (-12.0)

[a] ΔT_m = change in T_m's relative to unmodified reference duplexes. For experimental conditions, see Table 1. A/C/G/T = adenin-9-yl/cytosin-1-yl/guanin-9-yl/thymin-1-yl DNA monomers. LNA modifications are shown in lower case. See Figure 1 for structures of monomers **L**-**N**.

Binding specificity. Next, we evaluated the binding specificity of the modified ONs using DNA targets with mismatched nucleotides in the central position (Tables 3 and 4). As expected, reference strands **T1** and **A4** display excellent discrimination of mismatched targets. ONs with LNA nucleotides next to the mismatched region display improved binding specificity, while incorporation of LNA nucleotides as next-nearest neighbors is less beneficial (see ΔT_m's for **T1**-**T3**, Table 3, and **A4**-**A6**, Table 4), which is in line with previous reports.[24]

W1 and **X1**, which feature a central C5-ethynyl or C5-aminopropynyl modified 2′-deoxyuridine monomer, display similar binding specificity as reference strand **T1**, whereas singly pyrene-modified ONs **Y1** and **Z1** exhibit severely compromised binding specificity (see ΔT_m's for **B1** series, Table 3). Introduction of LNA nucleotides next to **W** or **X** monomers improves binding specificity relative to both LNA-free ONs (e.g., compare ΔT_m of **W2** relative to **W1**, Table 3) and LNA controls (e.g., compare ΔT_m of **W2** relative to **T2**, Table 3). The improvements are less pronounced when LNA nucleotides are positioned as next-nearest

neighbors, indicating that the beneficial influence of LNA monomers on binding specificity is short ranging[24] (e.g., compare ΔT_m of **W3** and **W2** relative to **W1**, Table 3). Introduction of LNA nucleotides near pyrene-functionalized monomers **Y** or **Z** does not compensate for the poor binding specificity of **Y**/**Z**-modified ONs (e.g., compare ΔT_m of **Y2** or **Y3** relative to **Y1**, Table 3).

Table 3. Discrimination of centrally mismatched DNA targets by ONs modified with C5-functionalized pyrimidine monomers **W**-**Z**.[a]

			DNA: 3′-CAC T**B**T ACG			
			T_m/°C	ΔT_m/°C		
ON	**Sequence**	**B** =	A	C	G	T
T1	5′-GTG ATA TGC		29.5	-16.5	-9.5	-17.0
W1	5′-GTG A**W**A TGC		31.0	-17.5	-11.5	-17.0
X1	5′-GTG A**X**A TGC		32.0	-15.0	-10.0	-16.5
Y1	5′-GTG A**Y**A TGC		22.5	+2.0	-3.0	-1.0
Z1	5′-GTG A**Z**A TGC		22.5	-8.0	-9.0	-4.0
T2	5′-GTG **a**T**a** TGC		38.5	-21.5	-14.5	-16.5
W2	5′-GTG **aWa** TGC		37.0	-21.0	-17.0	-16.0
X2	5′-GTG **aXa** TGC		41.0	-24.0	-19.5	-20.5
Y2	5′-GTG **aYa** TGC		23.5	-2.0	-4.0	-2.0
Z2	5′-GTG **aZa** TGC		21.5	-3.0	-8.0	-6.5
T3	5′-GT**g** ATA **t**GC		39.5	-17.5	-9.5	-15.5
W3	5′-GT**g** A**W**A **t**GC		37.5	-15.5	-10.0	-10.5
X3	5′-GT**g** A**X**A **t**GC		44.5	-19.5	-12.5	-12.5
Y3	5′-GT**g** A**Y**A **t**GC		26.0	+5.5	+1.5	+2.5
Z3	5′-GT**g** A**Z**A **t**GC		31.5	-9.0	-6.0	-2.0

[a] For experimental conditions, see Table 1. ΔT_m = change in T_m relative to fully matched duplex (**B** = A).

L4, featuring a single incorporation of C8-ethynyl modified 2′-deoxyadenosine **L**, has lower binding specificity than reference strand **A4** (Table 4). Incorporation of LNA nucleotides in the vicinity of monomer **L** results in improved discrimination of DNA targets with central A and G mismatches (compare ΔT_m of **L5** or **L6** relative to **L4**, Table 4). Incorporation of nearby LNA nucleotides does not substantially improve the poor binding specificity of **M**- or **N**-modified ONs, except when placed as next-nearest neighbors of monomer **N**.

Table 4. Discrimination of centrally mismatched DNA targets by ONs modified with C8-functionalized purine monomers **L**-**N**.[a]

			DNA: 3′-CGT A**B**A GTG			
			T_m/°C	ΔT_m/°C		
ON	**Sequence**	**B** =	T	A	C	G
A4	5′-GCA TAT CAC		29.5	-17.0	-15.5	-9.0
L4	5′-GCA T**L**T CAC		24.5	-10.5	-10.0	-10.0
M4	5′-GCA T**M**T CAC		17.5	-0.5	+3.5	-3.5
N4	5′-GCA T**N**T CAC		14.0	<-4.0	-0.5	-1.5
A5	5′-GCA **t**A**t** CAC		41.5	-20.0	-19.0	-18.0
L5	5′-GCA **tLt** CAC		36.0	-15.5	-10.5	-13.5
M5	5′-GCA **tMt** CAC		29.5	-1.5	-1.5	+0.5
N5	5′-GCA **tNt** CAC		29.0	-5.5	+5.5	-4.5
A6	5′-GC**a** TAT **c**AC		38.5	-16.0	-17.0	-16.0
L6	5′-GC**a** T**L**T **c**AC		34.0	-17.5	-10.5	-17.5
M6	5′-GC**a** T**M**T **c**AC		20.5	+7.5	+5.5	-2.5
N6	5′-GC**a** T**N**T **c**AC		17.0	<-7.5	<-7.5	<-7.5

[a] For experimental conditions, see Table 1. ΔT_m = change in T_m relative to fully matched duplex (**B** = T).

Photophysical characterization. Next, we set out to study if the presence of nearby LNA nucleotides influences the photophysical properties of pyrene-functionalized ONs. The UV-vis absorption spectra of single-stranded **Y1**-**Y3** show defined pyrene absorption maxima at ~375 nm and ~400 nm (Figure S2). Hybridization of **Y1** and **Y3** with cDNA/cRNA or centrally mismatched DNA targets results in bathochromic shifts of 2-6 nm (Table 5), which is indicative of strong interactions with neighboring nucleobases.[25] Interestingly, while hybridization of **Y2** with mismatched DNA targets also results in bathochromic shifts, binding with cDNA/cRNA does not, suggesting that flanking LNA nucleotides reduce pyrene-nucleobase interactions in matched duplexes. We speculate that this is due to LNA-mediated tuning of the duplex geometry and/or nucleobase orientation of monomer **Y** from *syn* to *anti*, resulting in a change of the pyrene binding mode from intercalation to major groove orientation.

Absorption maxima of ONs modified with C8-pyrenylethynyl DNA-A monomer **M** are observed at ~385 nm, ~400 nm and ~420 nm (Figure S3). Hybridization of **M4** with complementary or mismatched targets results in major bathochromic shifts (6-9 nm), whereas smaller, but still very prominent, shifts are observed for the LNA-modified **M5** or **M6** (Table 5).

Absorption spectra of ONs with incorporations of 3-(1-pyrenecarboxamido)propynyl monomers **Z** or **N** are broad, which precludes a detailed analysis of absorption maxima (Figures S4 and S5).

Table 5. Absorption maxima of pyrene-modified ONs in the presence or absence of complementary DNA/RNA (cDNA/cRNA) or centrally mismatched DNA targets.[a]

		λ_{max}/nm	$\Delta\lambda_{max}$/nm				
ON	**Sequence**	SSP	+cDNA	+cRNA	+MM C	+MM G	+MM T
Y1	5′-GTG A**Y**A TGC	396	+4	+2	+5	+4	+5
Y2	5′-GTG a**Y**a TGC	399	-2	+0	+3	+2	+4
Y3	5′-GTg A**Y**A tGC	395	+4	+2	+5	+4	+6
ON	**Sequence**	SSP	+cDNA	+cRNA	+MM A	+MM C	+MM G
M4	5′-GCA T**M**T CAC	412	+7	+7	+6	+7	+9
M5	5′-GCA t**M**t CAC	416	+3	+3	+3	+3	+3
M6	5′-GCa T**M**T cAC	416	+4	+4	+3	+0	+5

[a] Spectra were recorded in T_m buffer at T = 5 °C using each strand at 1 μM concentration. Targets for **Y**-series: 3′-[DNA]-CAC T**B**T ACG, where **B** = A (cDNA), C (MM C), G (MM G) or T (MM T), and 3′-[RNA]-CAC UAU ACG (cRNA). Targets for **M**-series: 3′-[DNA]-CGT A**B**A GTG, where **B** = T (cDNA), A (MM A), C (MM C) or G (MM G), and 3′-[RNA]-CGU AUA GUG (cRNA).

Steady-state fluorescence emission spectra of pyrene-modified ONs were recorded in the presence or absence of cDNA/cRNA or centrally mismatched DNA targets – spectra were recorded at 5 °C to maximize duplex formation. In line with literature reports,[14e] **Y**-modified ONs display broad emission profiles that are centered at 460 nm, which is indicative of strong electronic interactions between the pyrene and nucleobase moiety (Figure 2). Hybridization of **Y1** with cDNA/cRNA results in approximately 1.3- and 2.7-fold increased emission at 460 nm, respectively. Greater relative increases are observed when LNA nucleotides are incorporated as direct neighbors (approximately 2.0- and 4.5-fold increases for **Y2** vs cDNA and cRNA, respectively), whereas only minor emission differences are observed upon cDNA/cRNA hybridization for **Y3**, in which LNA nucleotides are positioned as next-nearest neighbors.

Proximal LNA nucleotides also influence how efficiently mismatched targets are discriminated via fluorescence. Thus, the fluorescence intensities of mismatched DNA duplexes involving **Y1** and **Y3** range from slightly lower to considerably greater than matched duplexes. In contrast, mismatched duplexes are consistently less emissive than matched duplexes when using **Y2**. This strongly suggests that flanking LNA nucleotides can be used to tune **Y**-modified ONs to yield probes with greater diagnostic potential. Similar trends are observed for 13-mer ONs, especially when monomer **Y** is flanked by ^{5Me}C or G LNA monomers (Figure S8), which are known quenchers of pyrene fluorescence.[14i,20]

ONs modified with 5-[3-(1-pyrenecarboxamido)propynyl]-2′-deoxyuridine monomer **Z** exhibit two broad fluorescence emission maxima at ~387 nm and ~406 nm (Figure 2).[14h,14i] Hybridization with cDNA/cRNA generally results in pronounced increases in fluorescence emission, especially with the LNA-containing probes. Thus, 11- and 9-fold increases in fluorescence intensity at 405 nm are observed for **Z2** upon cDNA/cRNA hybridization, while 3- and 7.5-fold increases are observed for **Z3**. Excellent mismatch discrimination is observed, especially for **Z2** where monomer **Z** is directly flanked by LNA monomers. We have explored the diagnostic potential of LNA-rich **Z**-modified probes in greater detail and found them to display distinct advantages over LNA-free probes, such as larger hybridization-induced increases in fluorescence emission, formation of more brightly fluorescent duplexes and improved SNP discrimination.[26] In fact, the properties of these probes closely resemble those of ONs modified with the corresponding 5-[3-(1-pyrenecarboxamido)propynyl] LNA-U monomer, which strongly suggests that the interesting fluorescent properties of C5-pyrene-functionalized LNA can be emulated by ONs in which nucleobase-modified DNA monomers are flanked by canonical LNA nucleotides.

It is important to stress that **Y**- and **Z**-modified probes discriminate between complementary and mismatched targets at non-stringent conditions, i.e., at conditions where mismatched duplexes are formed, which renders them as particularly promising SNP-discrimination probes. The pyrene moiety of monomer **Z** is hypothesized to point into the major groove in matched duplexes (limited interactions with nucleobases; blue-shifted absorbance; intense fluorescence emission; glycosidic torsion angle in the *anti* range), while being intercalated between base pairs in mismatched duplexes (pronounced interactions with flanking nucleobases; poor thermal mismatch discrimination; bathochromic shifts in pyrene absorption; quenched fluorescence; glycosidic torsion angle in *syn* range).[14h,14i] We speculate that the LNA monomers tune the furanose rings of proximal **Y** and **Z** monomers toward more pronounced *North*-type conformations, and thereby reduce the rotational freedom about the glycosidic angle of **Y** and **Z** due to steric interference between H3′ and H6 or the C5-substituent.[14i] This, in effect, results in greater positional control of the polarity-sensitive fluorophore and more distinct photophysical properties.

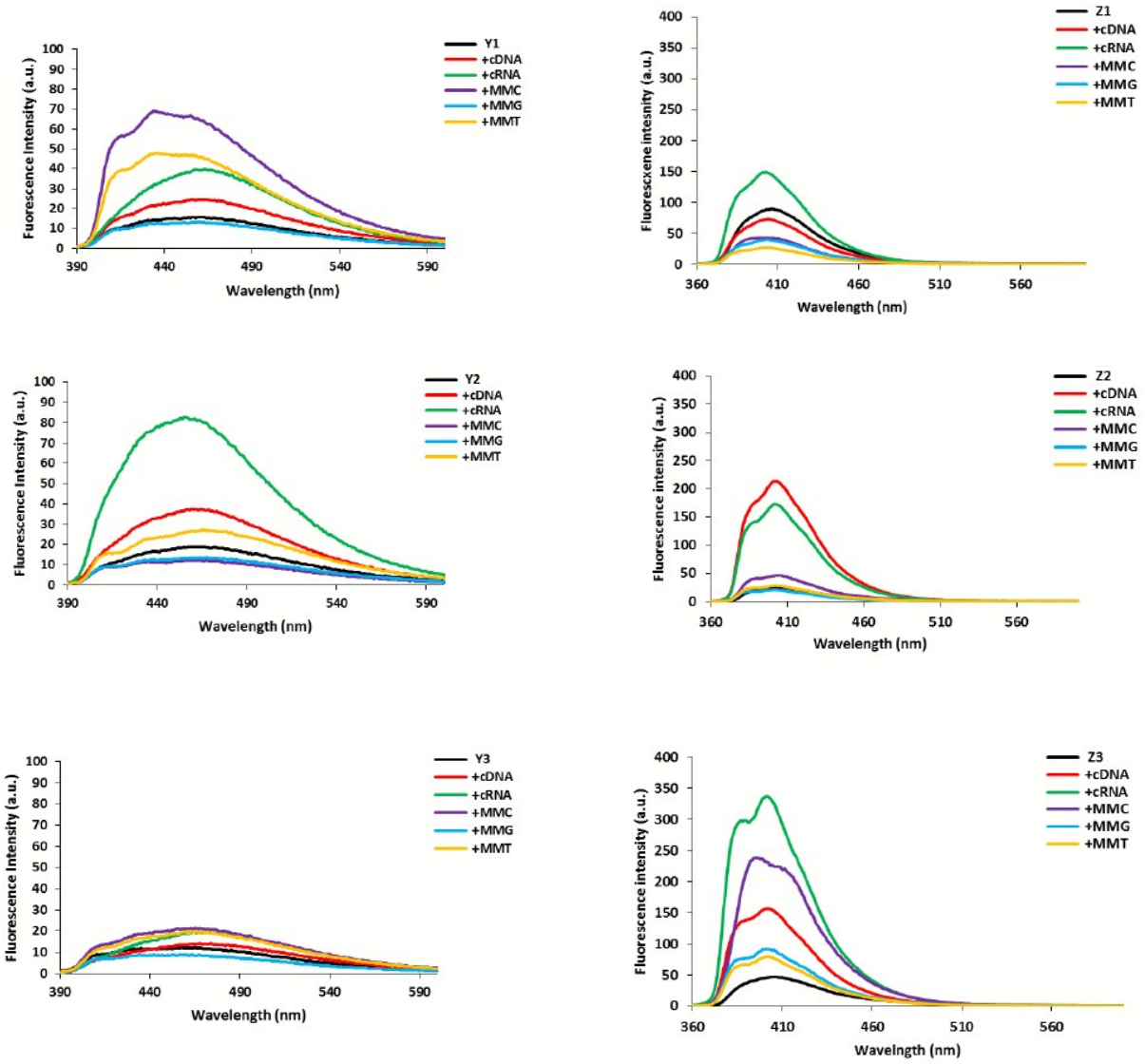

Figure 2. Steady-state fluorescence emission spectra of **Y1**-**Y3** or **Z1**-**Z3** in the presence or absence of complementary DNA/RNA (cDNA/cRNA) or centrally mismatched DNA targets (mismatched nucleoside specified) – for sequences of matched/mismatched targets, see footnote of Table 5. Spectra were recorded in T_m buffer at T = 5 °C using each strand at 1.0 μM and λ_{ex} = 380 nm and 340 nm for **Y**- and **Z**-modified ONs, respectively.

Steady-state fluorescence emission spectra of duplexes between **M4-M6** and complementary DNA/RNA or centrally mismatched DNA targets display a broad emission maximum centered around 460 nm (Figure 3).[14e] Hybridization of **M4** with cDNA/cRNA is accompanied by a ~1.5-fold increase in emission at ~460 nm, while the LNA-modified **M5** and **M6** display slightly more pronounced hybridization-induced increases in fluorescence intensity (~3- and ~2-fold, respectively). However, mismatched nucleotides opposite of monomer **M** are not efficiently discriminated via fluorescence, and these probes have limited potential for discrimination of single nucleotide polymorphisms (SNPs).

Fluorescence emission spectra of duplexes between **N4-N6** and complementary DNA/RNA or centrally mismatched DNA targets feature an emission maximum at ~410 nm with a shoulder at ~430 nm (Figure 3). Hybridization of **N4** or **N5** with matched or mismatched DNA targets only results in minor intensity changes, while duplex formation between **N6** and cDNA or cRNA is associated with ~4- and ~7-fold increases in emission levels, respectively. The highly quenched nature of the single-stranded **N6** is the primary reason for the large hybridization-induced increases in emission. However, mismatched targets are not discriminated efficiently via fluorescence.

To sum up, incorporation of flanking LNA monomers is an attractive strategy to improve the photophysical properties of ONs modified with C5-pyrene-functionalized 2′-deoxyuridine monomers, whereas the benefits are more limited with C8-pyrene-functionalized DNA monomers.

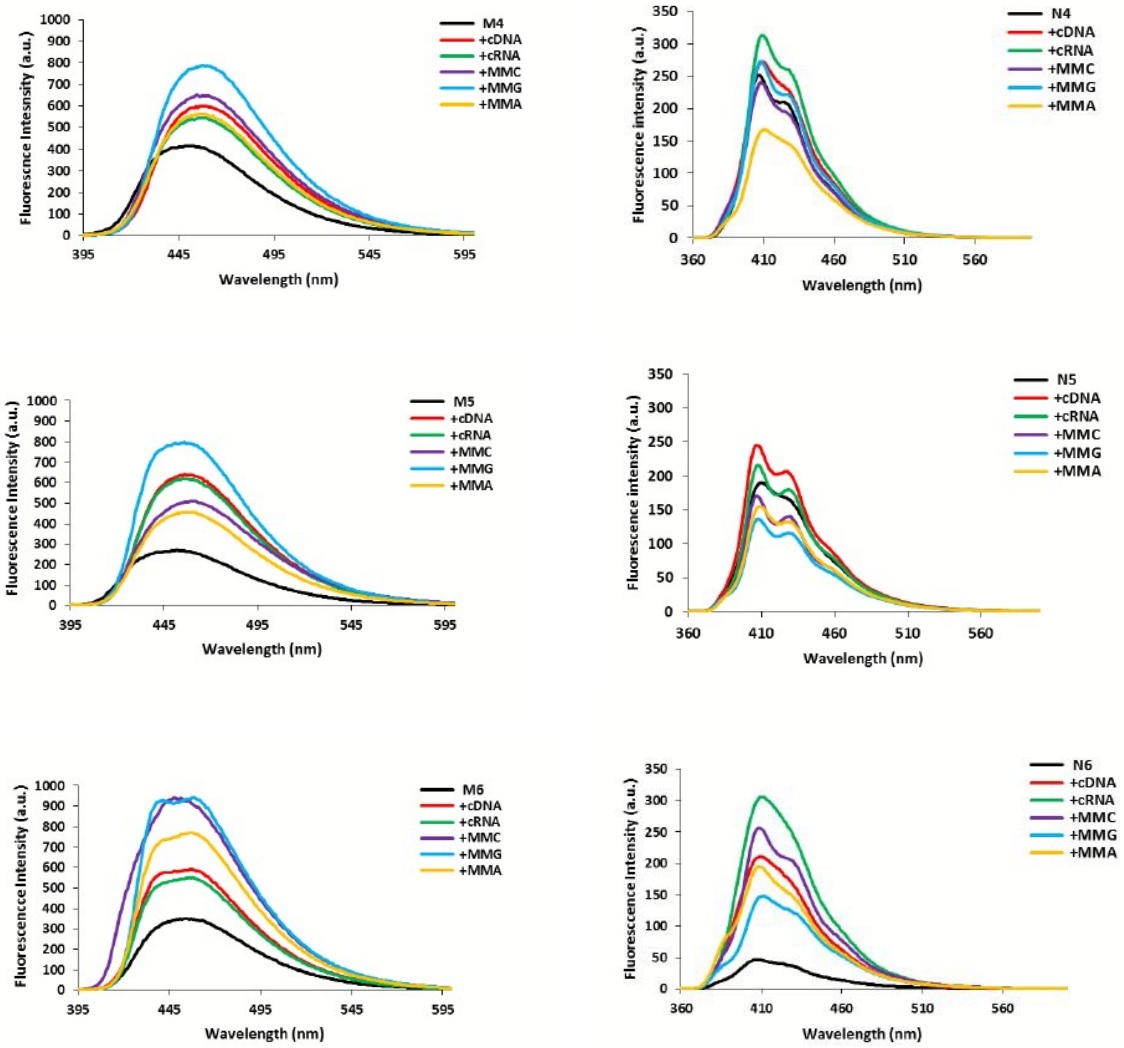

Figure 3. Steady-state fluorescence emission spectra of **M4**-**M6** or **N4**-**N6** in the presence or absence of complementary DNA/RNA (cDNA/cRNA) or centrally mismatched DNA targets (mismatched nucleoside is specified) – for sequences of matched/mismatched targets, see footnote of Table 5. Spectra were recorded in T_m buffer at T = 5 °C using each strand at 1.0 μM and λ_{ex} = 385 nm and 350 nm for **M**- and **N**-modified ONs, respectively.

CONCLUSION. Incorporation of LNA nucleotides next to C5-modified 2′-deoxyuridine or C8-modified 2′-deoxyadeonisine monomers almost invariably results in ONs with increased cDNA/cRNA affinity relative to corresponding LNA-free ONs. However, the effects on cDNA/cRNA affinity upon mixing monomers are not always additive, which renders it challenging to predict the hybridization properties of hybrid ONs[27] that are comprised of LNA[1-4] and nucleobase-modified DNA monomers.[14,15,28] Caution must therefore be exercised in assuming that mixmer ONs will exhibit hybridization properties that simply are the sum of monomer contributions.

Gratifyingly, the impact of LNA nucleotides on the photophysical properties of pyrene-functionalized ONs is more predictable. Thus, ONs in which LNA nucleotides directly flank C5-pyrene-functionalized 2′-deoxyuridine monomers **Y** and **Z**, display significantly increased fluorescence emission upon cDNA/cRNA binding and markedly improved fluorescent discrimination of mismatched targets at non-stringent conditions relative to the corresponding LNA-free probes. The enhanced photophysical characteristics are attributable to improved positional control of the pyrene moiety resulting from LNA-induced indirect conformational restriction of the pyrene moiety. LNA/C5-DNA hybrid ONs therefore present themselves as easy-to-synthesize alternatives to Glowing LNA[29] and other pyrene-functionalized oligonucleotide probes for applications in nucleic acid diagnostics.[14f,14h,28a,30-34]

EXPERIMENTAL SECTION

General experimental section. Reagents and solvents were obtained from commercial suppliers and of analytical grade and were used without further purification. Petroleum ether of the distillation range 60-80 °C was used. Dichloromethane, 1,2-dichloroethane, Et_3N and *N,N′*-diisopropylethylamine were dried over activated molecular sieves (4Å). Anhydrous pyridine and DMF were obtained from commercial sources. Reactions were conducted under argon whenever anhydrous solvents were used, and monitored by TLC using silica gel plates coated with a fluorescence indicator (SiO_2-60, F-254). Plates were visualized under UV light and by dipping in 5% conc. H_2SO_4 in absolute ethanol (v/v) followed by heating. Silica gel column chromatography was performed with silica gel 60 (particle size 0.040–0.063 mm) using moderate pressure (pressure ball). Columns on DMTr-protected nucleosides were built in the listed starting eluent containing 0.5% v/v pyridine. Evaporation of solvents was carried out under reduced pressure at temperatures below 45 °C. Following column chromatography, appropriate fractions were pooled, evaporated and dried at high vacuum for at least 12h to give the obtained products in high purity (>95%) as ascertained by 1D NMR techniques. Chemical shifts of ^{1}H NMR, ^{13}C NMR and ^{31}P NMR are reported relative to deuterated solvent or other internal standards (80% phosphoric acid for ^{31}P NMR). Exchangeable (ex) protons were detected by disappearance of ^{1}H NMR signals upon D_2O addition. Assignments of NMR spectra are based on 2D spectra (HSQC, COSY) and DEPT spectra. Quaternary carbons are not assigned in ^{13}C NMR but their presence was verified from HSQC and DEPT spectra (absence of signals). MALDI-HRMS spectra of compounds were recorded on a Q-TOF mass spectrometer using 2,5-dihydroxybenzoic acid as a matrix and a mixture of polyethylene glycol (PEG 600 or PEG 1000) as internal calibration standards. ESI-HRMS spectra were recorded in positive mode on a Q-TOF mass spectrometer; samples were dissolved in either CH_3CN or MeOH in 0.1% HCOOH.

6-*N*-Benzoyl-5′-*O*-(4,4′-dimethoxytrityl)-8-*C*-{3-(1-pyrenecarboxamido)propynyl}-2′-deoxyadenosine (2). Nucleoside **1**[19] (0.40 g, 0.54 mmol), $Pd(PPh_3)_4$ (63 mg, 0.05 mmol), CuI (21 mg, 0.11 mmol) and *N*-(prop-2-ynyl)pyrene-1-carboxamide[14h] (0.38 g, 1.35 mmol) were added to anhydrous DMF (10 mL) and the reaction chamber was degassed and placed under an argon atmosphere. To this was added anhydrous Et_3N (0.35 mL, 2.51 mmol) and the reaction mixture was stirred at 45 °C for ~3 h at which point solvents were evaporated off. The resulting residue was taken up in EtOAc (100 mL) and washed with brine (2×50 mL) and saturated aqueous $NaHCO_3$ (50 mL). The combined aqueous layer was then extracted with EtOAc (100 mL). The combined organic layers were dried (Na_2SO_4), evaporated to dryness and the resulting residue purified by column chromatography (0-5% MeOH in CH_2Cl_2, v/v) to afford nucleoside **2** (0.26 g, 50%) as a yellow solid material. R_f = 0.4 (5% MeOH in CH_2Cl_2, v/v); ESI-HRMS *m*/*z* 961.3293 ($[M+Na]^+$, $C_{58}H_{46}N_6O_7 \cdot Na^+$, Calc. 961.3326); ^{1}H NMR (500.1 MHz, DMSO-d_6) δ 11.26 (s, 1H, ex, NH), 9.41 (t, 1H, ex, J = 5.3 Hz, $NHCH_2$), 8.55-8.58 (m, 2H, Ar, H2), 8.10-8.38 (m, 8H, Ar), 8.05 (d, 2H, J = 7.5 Hz, Ar), 7.63-7.67 (m, 1H, Ar), 7.53-7.57 (m, 2H, Ar), 7.30-7.33 (m, 2H, Ar), 7.12-7.21 (m, 7H, Ar), 6.78 (d, 2H, J = 9.0 Hz, Ar), 6.75 (d, 2H, J = 9.0 Hz, Ar), 6.67 (m, 1H, H1′), 5.42 (d, 1H, ex, J = 4.5 Hz, 3′-OH), 4.71-4.76 (m, 1H, H3′), 4.61 (d, 2H, J = 5.3 Hz, CH_2NH), 4.06-4.10 (m, 1H, H4′), 3.70 (s, 3H, CH_3O), 3.68 (s, 3H, CH_3O), 3.34-3.40 (m, 1H, H2′), 3.22-3.29 (m, 2H, H5′), 2.35-2.41 (m, 1H, H2′); ^{13}C NMR (125.6 MHz, DMSO-d_6) δ 168.9, 165.5, 157.92, 157.90, 152.1 (C2), 151.1, 150.4, 144.9, 136.6, 135.7, 135.5, 133.2, 132.5 (Bz), 131.8, 130.7, 130.6, 130.1, 129.6 (DMTr), 128.50 (Ar), 128.45 (Ar), 128.41 (Ar), 128.3 (Ar), 127.9, 127.6 (DMTr), 127.5 (DMTr), 127.1 (Py), 126.6 (Py), 126.5 (DMTr), 125.9 (Py), 125.6 (Py), 125.3 (Py), 124.4 (Py), 123.8, 123.5, 113.0 (DMTr), 112.9 (DMTr), 95.4, 86.1

(C4′), 85.2, 84.9 (C1′), 71.0, 70.9 (C3′), 63.9 (C5′), 54.92 (CH_3O), 54.90 (CH_3O), 37.0 (C2′), 29.5 (CH_2NH).

5′-*O*-(4,4′-Dimethoxytrityl)-8-*C*-[2-(trimethylsilyl)ethynyl]-2′-deoxyadenosine (5L). Nucleoside **4**[21] (0.46 g, 0.73 mmol), $Pd(PPh_3)_4$ (84 mg, 0.07 mmol), CuI (28 mg, 0.15 mmol) and trimethylsilylacetylene (0.26 mL, 1.82 mmol) were added to anhydrous DMF (10 mL) and the reaction chamber was degassed and placed under an argon atmosphere. To this was added anhydrous Et_3N (0.42 mL, 3.00 mmol) and the reaction mixture was stirred at 50 °C for ~4 hr at which point solvents were evaporated off. The resulting residue was taken up in EtOAc (100 mL) and washed with brine (2×50 mL) and saturated aqueous $NaHCO_3$ (50 mL). The combined aqueous layer was then extracted with EtOAc (100 mL). The combined organic layer was dried (Na_2SO_4), evaporated to dryness, and the resulting residue purified by column chromatography (0-5% MeOH in CH_2Cl_2, v/v) to afford nucleoside **5L** (0.32 g, 68%) as an off-white solid material. R_f = 0.4 (5% MeOH in CH_2Cl_2, v/v); ESI-HRMS *m/z* 672.2626 ($[M+Na]^+$, $C_{36}H_{39}N_5O_5Si{\cdot}Na^+$, Calc. 672.2618); ^{1}H NMR (500.1 MHz, DMSO-d_6) δ 8.02 (s, 1H, H2), 7.49 (bs, 2H, ex, NH_2), 7.30-7.33 (m, 2H, DMTr), 7.14-7.22 (m, 7H, DMTr), 6.80 (d, 2H, J = 9.0 Hz, Ar), 6.76 (d, 2H, J = 9.0 Hz, Ar), 6.44 (dd, 1H, J = 7.0 Hz, 5.5 Hz, H1′), 5.33 (d, 1H, ex, J = 4.5 Hz, 3′-OH), 4.52-4.57 (m, 1H, H3′), 3.96-4.01 (m, 1H, H4′), 3.72 (s, 3H, CH_3O), 3.71 (s, 3H, CH_3O), 3.16-3.26 (m, 3H, H2′, 2×H5′), 2.25-2.31 (m, 1H, H2′), 0.24 (s, 9H, $(CH_3)_3Si$); ^{13}C NMR (125.6 MHz, DMSO-d_6) δ 157.93, 157.89, 155.9, 153.6 (C2), 148.5, 144.9, 135.7, 135.6, 132.5, 129.6 (DMTr), 129.5 (DMTr), 127.60 (DMTr), 127.56 (DMTr), 126.4 (DMTr), 119.0, 113.0 (DMTr), 112.9 (DMTr), 101.7, 93.8, 85.6 (C4′), 85.2, 83.9 (C1′), 70.9 (C3′), 64.0 (C5′), 54.95 (CH_3O), 54.93 (CH_3O), 37.0 (C2′), -0.77 ($(CH_3)_3Si$).

5′-*O*-(4,4′-Dimethoxytrityl)-8-*C*-[2-(1-pyrenyl)ethynyl]-2′-deoxyadenosine (5M). Nucleoside **4**[21] (200 mg, 0.32 mmol), $Pd(PPh_3)_4$ (40 mg, 0.03 mmol), CuI (12 mg, 0.06 mmol) and 1-ethynylpyrene[35] (143 mg, 0.63 mmol) were added to anhydrous DMF (5.0 mL) and the reaction chamber was degassed and placed under an argon atmosphere. To this was added anhydrous Et_3N (200 µL, 1.30 mmol) and the reaction mixture was stirred at 50 °C for ~ 4 h at which point solvents were evaporated off. The resulting residue was taken up in EtOAc (50 mL) and washed with brine (2×25 mL) and saturated aqueous $NaHCO_3$ (25 mL). The combined aqueous layer was extracted with EtOAc (50 mL). The combined organic layers were dried (Na_2SO_4), evaporated to dryness, and the resulting residue purified by column chromatography (0-5% MeOH in CH_2Cl_2, v/v) to afford nucleoside **5M** (200 mg, 80%) as a bright yellow solid material. R_f = 0.5 (6% MeOH in CH_2Cl_2, v/v); MALDI-HRMS *m/z* 800.2877 ($[M+Na]^+$, $C_{49}H_{39}N_5O_5{\cdot}Na^+$, Calc. 800.2849); ^{1}H NMR (500.1 MHz, DMSO-d_6) δ 8.60-8.63 (d, 1H, J = 9.0 Hz, Py), 8.27-8.46 (m, 7H, Py), 8.17-8.21 (t, 1H, J = 7.8 Hz, Py), 8.14 (s, 1H, H2), 7.59 (br s, 2H, ex, NH_2), 7.24-7.27 (m, 2H, DMTr), 7.08-7.14 (m, 7H, DMTr), 6.78 (dd, 1H, J = 7.5 Hz, 5.5 Hz, H1′), 6.63-6.67 (m, 4H, DMTr), 5.42 (d, 1H, ex, J = 5.0 Hz, 3′-OH), 4.69-4.74 (ap quintet, 1H, J = 5.7 Hz, H3′), 4.09 (ap q, 1H, J = 5.0 Hz, H4′), 3.614 (s, 3H, CH_3O), 3.606 (s, 3H, CH_3O), 3.52-3.59 (m, 1H, H2′), 3.15-3.19 (m, 2H, H5′), 2.43-2.49 (m, 1H, H2′); ^{13}C NMR (125.6 MHz, DMSO-d_6) δ 157.8, 156.0, 153.6 (C2), 148.9, 144.9, 135.7, 135.5, 133.5, 132.0, 131.8, 130.7, 130.3, 129.9 (Py), 129.5 (Ar), 129.2 (Py), 127.6 (DMTr), 127.5 (DMTr), 127.2 (Py), 127.0 (Py), 126.5 (Py), 126.4 (Ar), 126.3 (Ar), 125.0 (Py), 124.3 (Py), 123.5, 123.2, 119.5, 114.2, 112.83 (DMTr), 112.81 (DMTr), 93.4, 85.7 (C4′), 85.1, 84.8, 84.5 (C1′), 70.7 (C3′), 63.8 (C5′), 54.8 (CH_3O), 37.1 (C2′).

6-*N*-(Dimethylamino)methylene-5′-*O*-(4,4′-dimethoxytrityl)-8-*C*-ethynyl-2′-deoxyadenosine (6L). *N*,*N*-dimethylformamide dimethyl acetal (0.13 mL, 0.96 mmol) was added to a solution of nucleoside **5L** (0.25 g, 0.38 mmol) in anhydrous MeOH (5.0 mL) and the reaction mixture was stirred for 5 h at rt. All volatile components were evaporated and the resulting residue was taken up in ethyl acetate (50 mL) and subsequently washed with brine (2×25 mL) and saturated aqueous $NaHCO_3$ (25 mL). The organic layer was dried (Na_2SO_4), evaporated to dryness and the resulting residue purified by silica gel column chromatography (0-6% MeOH in CH_2Cl_2, v/v) to furnish nucleoside **6L** (200 mg, 83%) as an off-white solid material. R_f = 0.5 (6% MeOH in CH_2Cl_2, v/v); ESI-HRMS *m/z* 655.2653 ($[M+Na]^+$, $C_{36}H_{36}N_6O_5 \cdot Na^+$, calc. 655.2645); ^{1}H NMR (500.1 MHz, DMSO-d_6) δ 8.90 (s, 1H, $CH(NMe_2)$), 8.28 (s, 1H, H2), 7.27-7.30 (m, 2H, DMTr), 7.13-7.21 (m, 7H, DMTr), 6.78 (d, 2H, J = 9.0 Hz, DMTr), 6.73 (d, 2H, J = 9.0 Hz, DMTr), 6.48 (dd, 1H, J = 7.0 Hz, 6.0 Hz, H1′), 5.35 (br s, 1H, ex, 3′-OH), 5.00 (s, 1H, HC≡C), 4.61-4.68 (m, 1H, H3′), 3.98-4.03 (dd, 1H, J = 10.0 Hz, 4.5 Hz, H4′), 3.72 (s, 3H, CH_3O), 3.70 (s, 3H, CH_3O), 3.30-3.38 (m, 1H, H2′), 3.23 (s, 3H, CH_3N), 3.16-3.19 (m, 2H, H5′), 3.15 (s, 3H, CH_3N), 2.26-2.32 (m, 1H, H2′); ^{13}C NMR (125.6 MHz, DMSO-d_6) δ 157.91, 157.89 ($CH(NMe_2)$), 157.8, 152.3 (C2), 150.4, 144.9, 135.7, 135.6, 134.7, 129.6 (DMTr), 129.4 (DMTr), 127.6 (DMTr), 127.5 (DMTr), 126.4 (DMTr), 125.3, 112.93 (DMTr), 112.87 (DMTr), 87.7 (HC≡C), 85.8 (C4′), 85.1, 84.7 (C1′), 73.1, 70.8 (C3′), 63.7 (C5′), 54.92 (CH_3O), 54.89 (CH_3O), 40.8 (CH_3N), 36.5 (C2′), 34.7 (CH_3N).

6-*N*-(Dimethylamino)methylene-5′-*O*-(4,4′-dimethoxytrityl)-8-*C*-[2-(1-pyrenyl)ethynyl]-2′-deoxyadenosine (6M). *N*,*N*-dimethylformamide dimethyl acetal (0.18 mL, 1.35 mmol) was added to a solution of nucleoside **5M** (200 mg, 0.27 mmol) in anhydrous DMF (5.0 mL) and the reaction mixture was stirred at 50 °C for ~4 h. Volatile components were removed through evaporation and the resulting residue was taken up in ethyl acetate (50 mL) and washed with brine (2×25 mL) and saturated aqueous $NaHCO_3$ (25 mL). The organic layer was dried (Na_2SO_4), evaporated to dryness and the resulting residue purified by silica gel column chromatography (0-5% MeOH in CH_2Cl_2, v/v) to furnish nucleoside **6M** (190 mg, 87%) as a bright yellow solid material. R_f = 0.5 (6% MeOH in CH_2Cl_2, v/v); MALDI-HRMS *m/z* 855.3301 ($[M+Na]^+$, $C_{52}H_{44}N_6O_6 \cdot Na^+$, calc. 855.3271); ^{1}H NMR (500.1 MHz, DMSO-d_6) δ 8.95 (s, 1H, $CH(NMe_2)$), 8.65-8.68 (d, 1H, J = 9.0 Hz, Py), 8.29-8.47 (m, 8H, H2, Py), 8.20 (t, 1H, J = 7.5 Hz, Py), 7.24-7.27 (m, 2H, DMTr), 7.06-7.14 (m, 7H, DMTr), 6.83 (dd, 1H, J = 7.0 Hz, 5.5 Hz, H1′), 6.66 (d, 2H, J = 9.0 Hz, DMTr), 6.63 (d, 2H, J = 9.0 Hz, DMTr), 5.42 (d, 1H, ex, J = 5.0 Hz, 3′-OH), 4.71-4.75 (ap quintet, 1H, J = 5.4 Hz, H3′), 4.11 (ap q, 1H, J = 5.0 Hz, H4′), 3.609 (s, 3H, CH_3O), 3.605 (s, 3H, CH_3O), 3.54-3.59 (m, 1H, H2′), 3.26 (s, 3H, CH_3N), 3.17-3.22 (m, 5H, CH_3N, H5′), 2.48-2.51 (m, 1H, H2′ - overlap with DMSO-d_6 signal); ^{13}C NMR (125.6 MHz, DMSO-d_6) δ 159.1, 157.8, 157.7 ($CH(NMe_2)$), 152.7 (C2), 150.8, 144.8, 135.58, 135.55, 135.3, 132.0, 131.9, 130.7, 130.3, 130.0 (Py), 129.6 (Ar), 129.5, 129.4 (Ar), 129.3 (Ar), 127.55 (DMTr), 127.47 (DMTr), 127.2 (Py), 127.0 (Py), 126.52 (Py), 126.45 (Ar), 126.35 (Ar), 126.0, 125.0 (Py), 124.4 (Py), 123.5, 123.2, 114.0, 112.82 (DMTr), 112.79 (DMTr), 94.0, 85.8 (C4′), 85.1, 84.9, 84.6 (C1′), 70.7 (C3′), 63.8 (C5′), 54.8 (CH_3O), 40.7 (CH_3N), 37.0 (C2′), 34.7 (CH_3N).

Representative protocol for synthesis of phosphoramidites. Nucleosides **2**, **6L** and **6M** were dried through co-evaporation with anhydrous 1,2-dichloroethane (2×10 mL) and dissolved in anhydrous CH_2Cl_2. To this were added anhydrous *N*,*N*-diisopropylethylamine (DIPEA) and 2-cyanoethyl *N*,*N*-diisopropylchlorophosphoramidite (PCl reagent) (quantities and volumes specified below) and the reaction was stirred at rt for ~3.5 h when analytical TLC indicated complete conversion. The reaction mixture was diluted with CH_2Cl_2 (25 mL), washed with 5% aqueous $NaHCO_3$ (2×10 mL) and the combined aqueous layers back-extracted with CH_2Cl_2 (2×10 mL). The combined organic layers were dried (Na_2SO_4), evaporated to dryness, and the resulting residue purified by silica gel column chromatography (0-4% MeOH/CH_2Cl_2, v/v) and subsequent trituration from CH_2Cl_2 and petroleum ether to afford phosphoramidites **3L-3N**.

3′-*O*-[2-Cyanoethoxy(diisopropylamino)phosphinoxy]-6-*N*-(dimethylamino)methylene-5′-*O*-(4,4′-dimethoxytrityl)-8-*C*-ethynyl-2′-deoxyadenosine (3L). Nucleoside **6L** (220 mg, 0.35 mmol) in anhydrous CH_2Cl_2 (5 mL), DIPEA (0.24 mL, 1.40 mmol) and PCl reagent (0.18 mL, 0.77 mmol) were mixed, reacted, worked up and purified as described above to provide phosphoramidite **3L** (210 mg, 72%) as a white foam. R_f = 0.5 (2% MeOH in CH_2Cl_2, v/v); MALDI-HRMS *m/z* 855.3746 ($[M+Na]^+$, $C_{45}H_{53}N_8O_6P{\cdot}Na^+$, calc. 855.3723); ^{31}P NMR (121.5 MHz, $CDCl_3$) δ 148.9, 148.6.

3′-*O*-[2-Cyanoethoxy(diisopropylamino)phosphinoxy]-6-*N*-(dimethylamino)methylene-5′-*O*-(4,4′-dimethoxytrityl)-8-*C*-[2-(1-pyrenyl)ethynyl]-2′-deoxyadenosine (3M). Nucleoside **6M** (250 mg, 0.30 mmol) in anhydrous CH_2Cl_2 (5 mL), DIPEA (0.16 mL, 1.20 mmol) and PCl reagent (0.15 mL, 0.66 mmol) were mixed, reacted, worked up and purified as described above

to provide phosphoramidite **3M** (200 mg, 64%) as a white foam. R_f = 0.5 (2% MeOH in CH_2Cl_2, v/v); MALDI-HRMS *m/z* 1055.4387 ($[M+Na]^+$, $C_{61}H_{61}N_8O_6P{\cdot}Na^+$, calc. 1055.4349); ^{31}P NMR (121.5 MHz, $CDCl_3$) δ 149.1, 148.7.

6-*N*-Benzoyl-3′-*O*-[2-cyanoethoxy(diisopropylamino)phosphinoxy]-5′-*O*-(4,4′-dimethoxytrityl)-8-*C*-[3-(1-pyrenecarboxamido)propynyl]-2′-deoxyadenosine (3N). Nucleoside **2** (0.32 g, 0.34 mmol) in anhydrous CH_2Cl_2 (5 mL), DIPEA (0.24 mL, 1.36 mmol) and PCl reagent (0.17 mL, 0.75 mmol) were mixed, reacted, worked up and purified as described above to provide phosphoramidite **3N** (233 mg, 60%) as a white foam. R_f = 0.5 (2% MeOH in CH_2Cl_2, v/v); MALDI-HRMS *m/z* 1161.4421 ($[M+Na]^+$, $C_{67}H_{63}N_8O_8P{\cdot}Na^+$, calc. 1161.4404); ^{31}P NMR (121.5 MHz, $CDCl_3$) δ 148.6, 148.5.

Synthesis and purification of ONs. ONs were prepared on a DNA synthesizer (0.2 μmol scale) using succinyl linked LCAA-CPG (long chain alkyl amine controlled pore glass) columns with 500Å pore size. Standard protocols for incorporation of DNA phosphoramidites were used. A ~50-fold molar excess of modified phosphoramidites in anhydrous dichloromethane (0.05 M) was used along with extended oxidation (45s) and hand-coupling, which resulted in coupling yields greater than 95% (20 min, 5-(ethylthio)-1*H*-tetrazole as activator for incorporation of monomers **M** and **N**; 20 min, 4,5-dicyanoimidazole as activator for incorporation of monomers **W/X//L;** 20 min, 5-(bis-3,5-trifluromethylphenyl)-1H-tetrazole, for incorporation of monomers **Y** and **Z**). Cleavage from solid support and removal of nucleobase protecting groups was accomplished using 32% aqueous ammonia (55 °C, ~18h). Crude 5′-DMTr-ONs were purified on HPLC (XTerra MS C18 column) using a 0.05 mM triethylammonium acetate buffer - 25%

water/acetonitrile (v/v) gradient. Purified ONs were detritylated using 80% aqueous AcOH (20 min) and precipitated (NaOAc/$NaClO_4$/acetone, -18 °C). The identity of the synthesized ONs was verified through MS analysis recorded in positive ion mode on a quadrupole time-of-flight tandem mass spectrometer equipped with a MALDI source using anthranilic acid as a matrix (Table S1), while purity (>80% for **L/M/W/X/Y**-modified ONs and ≥75% for **N/Z**-modified ONs) was verified by ion-pair reverse phase HPLC running in analytical mode.

Thermal denaturation experiments. ON concentrations were estimated using the following extinction coefficients (OD/μmol) for DNA: dG (12.01), dA (15.20), T (8.40), dC (7.05); for RNA: rG (13.70), rA (15.40), U (10.00), rC (9.00); and for pyrene (22.4). The strands comprising a given duplex were mixed and annealed. Thermal denaturation temperatures of duplexes (1.0 μM final concentration of each strand) were determined using a temperature-controlled UV/vis spectrophotometer and quartz optical cells with 1.0 cm path lengths. T_m's were determined as the first derivative maximum of thermal denaturation curves (A_{260} vs. T) recorded in medium salt buffer (100 mM NaCl, 0.1 mM EDTA, pH 7.0 adjusted with 10 mM NaH_2PO_4 and 5 mM Na_2HPO_4). The temperature of the denaturation experiments ranged from at least 15 °C below T_m to 20 °C above T_m (although not below 5 °C). A temperature ramp of 0.5 °C/min was used in all experiments. Reported T_m's are reported as averages of two experiments within ± 1.0 °C.

Absorption spectroscopy. UV-vis absorption spectra were recorded at 5 °C using the same samples and instrumentation as in thermal denaturation experiments.

Fluorescence spectroscopy. Steady-state fluorescence emission spectra were recorded in non-deoxygenated thermal denaturation buffer (each strand used in 1.0 μM concentration) using an excitation wavelength of λ_{ex} = 380 nm, 340 nm, 385 nm and 350 nm for **Y**-, **Z**-, **M**- and **N**-modified ONs, respectively, and excitation slit 5.0 nm, emission slit 5.0 nm and a scan speed of 600 nm/min. Experiments were performed at temperature (~5 °C).

ACKNOWLEDGEMENTS. This work was supported by Idaho NSF EPSCoR, the BANTech Center at the Univ. of Idaho, and The Office of Naval Research (Research Opportunity Number ONR BAA 09-022). We thank Dr. Alexander Blumenfeld (Dept. Chemistry), and Dr. Lee Deobald (EBI Murdock Mass Spectrometry Center, Univ. Idaho) for NMR and mass spectrometric analyses.

NOTES AND REFERENCES.

† Electronic supplementary information (ESI) available: MS data for new modified ONs; representative T_m curves; additional thermal denaturation, absorption and fluorescence data.

1) S. K. Singh, P. Nielsen, A. A. Koshkin and J. Wengel, *Chem*. *Commun*., 1998, 455-456.

2) S. Obika, D. Nanbu, Y. Hari, J.-I. Andoh, K.-I. Morio, T. Doi and T. Imanishi, *Tetrahedron Lett*., 1998, **39**, 5401-5404.

3) H. Kaur, B. R. Babu and S. Maiti, *Chem*. *Rev*., 2007, **107**, 4672-4697.

4) J. K. Watts, *Chem*. *Commun*., **2013**, *49*, 5618-5620.

5) For recent reviews see: a) S. Obika, S. M. A. Rahman, A. Fujisaka, Y. Kawada, T. Baba and T. Imanishi, *Heterocycles*, 2010, **81**, 1347-1392; b) C. Zhou and J. Chattopadhyaya, *Chem*. *Rev*.,

2012, **112**, 3808-3832; c) P. P. Seth and E. E. Swayze in *Natural Products in Medicinal Chemistry*, 1st Ed. (Ed: S. Hanessian), Wiley-VCH, Weinheim, 2014, 403-439.

6) For recent representative examples see: a) S. Hanessian, J. Wagger, B. L. Merner, R. D. Giacometti, M. E. Østergaard, E. E. Swayze and P. P. Seth, *J. Org. Chem*., 2013, **78**, 9064-9075. b) N. K. Andersen, B. A. Anderson, J. Wengel and P. J. Hrdlicka, *J. Org. Chem*., 2013, **78**, 12690-12702. c) S. Kumar, S. I. Steffansen, N. Albæk and P. Nielsen, *Tetrahedron* 2014, **70**, 583-589. d) C. Lou, B. Vester and J. Wengel, *Chem. Commun*., 2015, **51**, 4024-4027. e) Y. Hari, T. Morikawa, T. Osawa and S. Obika, *Org. Lett*., 2013, **15**, 3702-3705. f) A. R. Shrestha, Y. Kotobuki, Y. Hari and S. Obika, *Chem. Commun*., 2014, **50**, 575-577. g) Y. Mitsuoka, Y. Fujimura, R. Waki, A. Kugimiya, T. Yamamoto, Y. Hari and S. Obika, *Org. Lett*., 2014, **16**, 5640-5643. h) T. Yamamoto, A. Yahara, R. Waki, H. Yasuhara, F. Wada, M. Harada-Shiba and S. Obika, *Org. Biomol. Chem*., 2015, **13**, 3757-3765.

7. a) P. Kumar, M. E. Østergaard, B. Bharal, B. A. Anderson, D. C. Guenther, M. Kaura, D. J. Raible, P. K. Sharma and P. J. Hrdlicka, *J. Org. Chem*., 2014, **79**, 5047-5061. b) M. Kaura, D. C. Guenther and P. J. Hrdlicka, *Org. Lett*., 2014, **16**, 3308-3311. c) D. C. Guenther, P. Kumar, B. A. Anderson and P. J. Hrdlicka, *Chem. Commun*., 2014, **50**, 9007-9009.

8) K. Morihiro, O. Hasegawa, S. Mori, S. Tsunoda and S. Obika, *Org. Biomol. Chem*., 2015, DOI: 10.1039/C5OB00477B.

9) M. Kaura, P. Kumar and P. J. Hrdlicka, *J. Org. Chem*., 2014, **79**, 6256-6268.

10) a) M. Petersen, C. B. Nielsen, K. E. Nielsen, G. A. Jensen, K. Bondensgaard, S. K. Singh, V. K. Rajwanshi, A. A. Koshkin, B. M. Dahl, J. Wengel and J. P. Jacobsen, *J. Mol. Recognit*., 2000, **13**, 44-53. b) K. Bondensgaard, M. Petersen, S. K. Singh, V. K. Rajwanshi, R. Kumar, J. Wengel and J. P. Jacobsen, *Chem. Eur. J*., **2000**, *6*, 2687-2695. c) M. Egli, G. Minasov, M. Teplova, R.

Kumar and J. Wengel, *J. Chem. Soc. Chem. Commun*., 2001, **7**, 651-652. d) K. E. Nielsen and H. P. Spielmann, *J. Am. Chem. Soc*., 2005, **127**, 15273-15282.

11) a) N. Kalra, B. R. Babu, V. S. Parmar and J. Wengel, *Org. Biomol. Chem*., 2004, **2**, 2885-2887. b) N. Kalra, M. C. Parlato, V. S. Parmar and J. Wengel, *Bioorg. Med. Chem. Lett*., 2006, **16**, 3166-3169.

12) I. V. Astakhova, A. V. Ustinov, V. A. Korshun and J. Wengel, *Bioconjugate Chem*., 2011, **22**, 533-539.

13) S. Karmakar and P. J. Hrdlicka, *Chem. Sci*., 2013, **4**, 3447-3454.

14) a) J. Sagi, A. Szemzo, K. Ebinger, A. Szabolcs, G. Sagi, E. Ruff and L. Otvos, *Tetrahedron Lett*., 1993, **34**, 2191-2194. b) D. Graham, J. A. Parkinson and T. Brown, *J. Chem. Soc. Perkin Trans. 1*, 1998, 1131-1138. c) L. E. Heystek, H. Q. Zhou, P. Dande and B. Gold, *J. Am. Chem. Soc*., 1998, **120**, 12165-12166. d) J. Booth, T. Brown, S. J. Vadhia, O. Lack, W. J. Cummins, J. O. Trent and A. N. Lane, *Biochemistry*, 2005, **44**, 4710-4719. e) E. Mayer, L. Valis, C. Wagner, M. Rist, N. Amann and H.-A. Wagenknecht, *ChemBioChem*, 2004, **5**, 865-868. f) G. T. Hwang, Y. J. Seo, S. J. Kim and B. H. Kim, *Tetrahedron Lett*., 2004, **45**, 3543-3546. g) M. V. Skorobogatyi, A. D. Malakhov, A. A. Pchelintseva, A. A. Turban, S. L. Bondarev and V. A. Korshun, *ChemBioChem*, 2006, **7**, 810-816. h) A. Okamoto, K. Kanatani and I. Saito, *J. Am. Chem. Soc*., 2004, **126**, 4820-4827. i) M. E. Østergaard, P. Kumar, B. Baral, D. C. Guenther, B. A. Anderson, F. M. Ytreberg, L. Deobald, A. J. Paszczynski, P. K. Sharma and P. J. Hrdlicka, *Chem. Eur. J*., 2011, **17**, 3157-3165.

15) Thermal denaturation properties of ONs modified with monomers **L** or **N** have - to the best of our knowledge - not been previously reported. The closest analogs of **L**-modified ONs are ONs modified with 8-vinyl 2′-deoxyadenosine, 8-propynyl 2′-deoxyadenosine or 7-ethynyl-7-

deaza-2′-deoxyadenosine reported in reference 14b and: a) B. Catalanotti, A. Galeone, L. Gomez-Paloma, L. Mayola and A. Pepe, *Bioorg. Med. Chem. Lett.*, 2000, **10**, 2005-2009. b) N. B. Gaied, N. Glasser, N. Ramalanjaona, H. Beltz, P. Wolff, R. Marquet, A. Burger and Y. Mely, *Nucleic Acids Res.*, 2005, **33**, 1031-1039. c) F. Seela and M. Zulauf, *Helv. Chim. Acta*, **1999**, *82*, 1878-1898.

16) a) F. Diezmann, H. Eberhard and O. Seitz, *Pept. Sci.*, 2010, **94**, 397-404. b) K. A. Cruickshank and D. L. Stockwell, *Tetrahedron Lett.*, 1988, **29**, 5221-5224.

17) A. D. Malakhov, E. V. Malakhova, S. V. Kuznitsova, I. V. Grechishnikova, I. A. Prokhorenko, M. V. Skorobogatyi, V. A. Korshun, and Y. A. Berlin, *Russ. J. Bioorg. Chem.*, 2000, **26**, 34-44.

18) The final O3′-phosphitylation step in the synthesis of the corresponding phosphoramidites of the C5-functionalized 2′-deoxyuridine monomers **W**-**Z** was carried out using 2-cyanoethyl-*N*,*N*-diisopropylchlorophosphoramidite and DIPEA in CH_2Cl_2.

19) M. T. Tierney and M. W. Grinstaff, *Org. Lett.*, 2000, **2**, 3413-3416.

20) Y. J. Seo, J. H. Ryu and B. H. Kim, *Org. Lett.*, 2005, **7**, 4931-4933.

21) L. Clima and W. Bannwarth, *Helv. Chim. Acta*, 2008, **91**, 165-175.

22) G. S. Ti, B. L. Gaffney and R. A. Jones, *J. Am. Chem. Soc.*, 1982, **104**, 1316-1319.

23) L. J. McBride, R. Kierzek, S. L. Beaucage and M. H. Caruthers, *J. Am. Chem. Soc.*, 1986, **108**, 2040-2048.

24) Y. You, B. G. Moreira, M. A. Behlke and R. Owczarzy, *Nucleic Acids Res.*, 2006, **34**, e60.

25) H. Asanuma, T. Fujii, T. Kato and H. Kashida, *J. Photochem. Photobiol. C.*, 2012, **13**, 124-135.

26) M. Kaura and P. J. Hrdlicka, manuscript in preparation.

27) C. Ahlborn, K. Siegmund and Clemens Richert, *J. Am. Chem. Soc.*, 2007, **129**, 15218-15232.

28) a) A. Okamoto, Y. Saito and I. Saito. *J. Photochem. Photobiol. C: Photochem. Rev.*, 2005, **6**, 108-122. b) M. Ahmadian and D. E. Bergstrom in *Modified Nucleotides in Biochemistry, Biotechnology and Medicine*, 1st Ed (Ed: P. Herdewijn), Wiley-VCH, Weinheim, 2008, 251-276. c) R. W. Sinkeldam, N. J. Greco and Y. Tor, *Chem. Rev.*, 2010, **110**, 2579-2619. d) W. Schmucker and H.-A. Wagenknecht, *Synlett*, 2012, **23**, 2435-2448. e) A. Matarazzo and R. H. E. Hudson, *Tetrahedron*, 2015, **71**, 1627-1657.

29) a) P. J. Hrdlicka, B. R. Babu, M. D. Sørensen, N. Harrit and J. Wengel, *J. Am. Chem. Soc.*, 2005, **127**, 13293-13299. b) M. E. Østergaard, P. Cheguru, M. R. Papasani, R. A. Hill and P. J. Hrdlicka, *J. Am. Chem. Soc.*, 2010, **132**, 14221-14228.

30) K. Yamana, H. Zako, K. Asazuma, R. Iwase, H. Nakano and A. Murakami, *Angew. Chem., Int. Ed.*, 2001, **40**, 1104-1106.

31) I. V. Astakhova, V. A. Korshun and J. Wengel, *Chem. Eur. J.*, 2008, **14**, 11010-11026.

32) I. V. Astakhova, D. Lindegaard, V. A. Korshun and J. Wengel, *Chem. Commun.*, 2010, **46**, 8362-8364.

33) M. E. Østergaard, D. C. Guenther, P. Kumar, B. Baral, L. Deobald, A. J. Paszczynski, P. K. Sharma and P. J. Hrdlicka, *Chem. Commun.*, 2010, 4929-4931.

34) M. E. Østergaard and P. J. Hrdlicka, *Chem. Soc. Rev.*, 2011, **40**, 5771-5788.

35) W. Wu, W. Wu, S. Ji, H. Guo and J. Zhao, *Eur. J. Inorg. Chem.*, 2010, 4470-4482.